Lung Cancer 132 (2019) 132–140

Contents lists available at ScienceDirect

Lung Cancer

journal homepage: www.elsevier.com/locate/lungcan

Cause-and-Effect relationship between FGFR1 expression and epithelial-mesenchymal transition in *EGFR*-mutated non-small cell lung cancer cells

Johan Vad-Nielsen, Kristine Raaby Gammelgaard, Tina Fuglsang Daugaard, Anders Lade Nielsen*

Department of Biomedicine, Aarhus University, Aarhus, Denmark

ARTICLE INFO

Keywords:
NSCLC
EMT
CRISPR-dCAS9
EGFR
FGFR1
ZEB1

ABSTRACT

Objectives: Increased FGFR1 expression is associated with resistance to tyrosine kinase inhibitors (TKIs) in *EGFR*-mutated NSCLC cells and often concomitant with epithelial to mesenchymal transition (EMT). However, the cause-and-effect relationship between increased FGFR1 expression and EMT in the genetic background of *EGFR*-mutated non-small cell lung cancer (NSCLC) cells is not clear. Previous studies have specifically addressed the relationship between EMT and increased FGFR1 expression in the context of simultaneous TKI-mediated blocking of EGFR-signaling. Here, in the context of *EGFR*-mutated NSCLC cells with active EGFR-signaling, we have examined whether increased FGFR1 expression drives EMT or is an EMT passenger event.

Materials and methods: For cause-and-effect analyses between EMT and FGFR1 expression, including expression of alternative spliced FGFR1 isoforms, we used CRISPR-dCAS9-SAM-mediated induction of the endogenous *FGFR1* and *ZEB1* genes, as well as biochemical EMT-induction, in PC9 and HCC827 NSCLC cell lines harboring activating *EGFR*-mutations.

Results: We find that *FGFR1* expression correlates with a *ZEB1*-associated EMT gene expression profile in NSCLC cells. In experiments using NSCLC cell lines harboring activating *EGFR*-mutations we show that CRISPR-dCAS9-SAM-mediated induction of *FGFR1* expression is neither driving an increase in *ZEB1* expression nor EMT characteristics. However, CRISPR-dCAS9-SAM-mediated induction of *ZEB1* expression drives EMT characteristics and an increase in *FGFR1* expression. Biochemical induction of EMT also drives an increase in *FGFR1* expression.

Conclusion: From our findings concerning the cause-and-effect relationship in the genetic background of *EGFR*-mutated NSCLC cells, we conclude that an increase in *ZEB1* expression is a driver of EMT resulting in concomitant increased *FGFR1* expression, whereas an increase in *FGFR1* expression is insufficient to drive concomitant EMT.

1. Introduction

Lung cancer remains the leading cause of cancer-related death worldwide, with a disappointing five-year survival rate of approximately 15% [1]. Due to the advanced stage at the time of diagnosis, the prognosis is often poor, and therapeutic options are limited. The presence of multiple metastases renders surgical resection inadequate, and resistance to treatment is a growing problem. Non-small cell lung cancer (NSCLC) represents the most common group of lung cancer (approximately 80% of cases), and activating mutations in receptor tyrosine kinases (RTKs), *e.g.*, in the Epidermal Growth Factor Receptor (*EGFR*) gene, are frequently observed driver mutations in NSCLC [2]. Hence, EGFR has been a target of treatment with the use of tyrosine kinase inhibitors (TKIs) such as erlotinib and gefitinib, which in particular efficiently target EGFR presented with activating mutations [3–6]. Despite the initial efficacy of TKI treatment, all patients with activating *EGFR*-mutations acquire TKI resistance over time [4,7,8].

A mechanism that has received increasing attention for its role in cancer drug resistance is epithelial to mesenchymal transition (EMT) [9,10]. EMT is a shift in the cell differentiation program governed by members of the EMT transcription factor (EMT-TF) families TWIST, SNAI and ZEB. EMT involves the disruption of cell-cell adherence and tight junctions as well as loss of cell polarity of epithelial cells with a resulting acquisition of a mesenchymal-like phenotype [11,12]. EMT mediates increased cancer cell invasive potential and thereby supports tumor metastasis. Moreover, EMT is frequently accompanied by cancer drug resistance both *in vitro* and *in vivo* in pancreatic cancer [13], bladder cancer [14], and breast cancer [15]. In NSCLC, EMT is reported

* Corresponding author at: Department of Biomedicine, Aarhus University, DK-8000, Aarhus C, Denmark.
E-mail address: aln@biomed.au.dk (A.L. Nielsen).

https://doi.org/10.1016/j.lungcan.2019.04.023
Received 7 January 2019; Received in revised form 15 April 2019; Accepted 18 April 2019

to predict sensitivity to EGFR-TKIs [16] and is associated with acquired resistance to EGFR-TKI treatment of *EGFR*-mutated cancer cells [17–21]. However, the detailed molecular basis for the onset of EMT in acquired EGFR-TKI resistance in *EGFR*-mutated NSCLC cells remains elusive.

The fibroblast growth factor receptor family (FGFR1-4) belongs to the RTK family and is involved in many physiological processes, including embryogenesis, angiogenesis, and wound repair [22]. Dysregulation of FGFR1 is reported in a broad range of malignancies leading to tumorigenesis, transformation, and tumor progression [23,24]. In a subset of *EGFR*-mutated NSCLC cells with acquired EGFR-TKI resistance, FGFR1 expression is increased, and such resistant cells are sensitive to FGFR1 inhibitors [17,25,26]. Activation of an autocrine FGF2-FGFR1 loop causes EGFR-TKI resistance through bypassing of downstream PI3K/AKT and MEK/ERK signaling blockade [17,20,25,26]. In addition, FGFR1-mediated bypass signaling provides intrinsic resistance to TKIs in NSCLC cells harboring *EGFR*-mutations [27].

Increased FGFR1 expression is reported to be associated with EMT in cancer cells from a variety of different tissues, and activation of FGFR1 is described as having the capability to promote EMT in breast cancer [28], prostate cancer [29], and *FGFR1*-amplified lung cancer [30]. A recurrently observed type of TKI resistant *EGFR*-mutated NSCLC cells is presented with EMT and increased FGFR1 expression as concomitant events [17,20,25]. FGFR1 inhibition restores sensitivity to EGFR-TKIs in the acquired resistant EMT *EGFR*-mutated cells without reverting the EMT phenotype [17,20]. However, the cause-and-effect relationship between increased *FGFR1* expression and the onset of EMT in the genetic background of *EGFR*-mutated NSCLC cells is still not clear. A limitation of previous studies is the systematic inclusion of the simultaneous blocking of EGFR-signaling by TKIs. Here we have investigated the cause-and-effect relationship between increased FGFR1 expression and the onset of EMT in the genetic background of *EGFR*-mutated NSCLC cells without TKIs simultaneously interfering with EGFR-signaling. Our findings show that increased FGFR1 expression does not result in EMT, whereas EMT results in increased FGFR1 expression.

2. Material and methods

2.1. Cell culture

HCC827 (ATCC/LCG, Wesel, Germany) and PC9 (PHE culture collection, Salisbury, UK) cell lines were grown in RPMI supplemented with 10% fetal calf serum and 1% Penicillin-streptomycin (Gibco, Thermo Fischer Scientific, Waltham, MA, USA) at 37 °C and 5% CO_2. HCC827 and PC9 cell lines harbor an *EGFR* exon19del E746–A750 mutation, rendering EGFR constitutively active. The previously established HCC827 erlotinib resistant (ER) cell clones used in this work are HCC827 ER clones 4, 7, and 10 [17]. These cell clones were characterized to have an EMT-induced mesenchymal phenotype [17]. The HCC827 ER cell clones were grown in presence of 5μM erlotinib.

2.2. CRISPR-dCAS9 NSCLC cell lines

Expression of endogenous *ZEB1* and *FGFR1* genes was induced using a modified version of the CRISPR-dCas9 synergistic activation mediator (SAM) approach [27,31,32]. Briefly summarized, PC9 and HCC827 cells were initially transduced with a CRISPR-dCas9 expression cassette and subsequently stable transfected with a multiplexed gRNA PiggyBag transposon expression vector with three unique gRNAs spanning the promoter region of either *FGFR1* (gFGFR1) or ZEB1 (gZEB1) [27,31]. Control cells were generated by transfection with the gRNA expression vector with *mCherry* gRNA inserted in three repetitions (gCTR) [27]. We previously described the CRISPR-dCas9-SAM method for inducing *FGFR1* expression in PC9 and HCC827 cell lines including the gRNA sequences for *FGFR1* and *mCherry* [27]. We have also previously demonstrated the activity of the gRNA sequences for *ZEB1* in transiently transfected breast cancer cells [31]. To maintain expression of the various CRISPR-dCas9-SAM components the cell lines were grown with blasticidin (0.5 μg/mL, Gibco), hygromycin (200 μg /mL, Life Technologies), and puromycin (1 μg/mL for PC9 and 0.5 μg/mL for HCC827).

2.3. Reverse transcriptase quantitative PCR (RT-qPCR)

For RNA extraction was used TRI Reagent according to manufacturer's instructions (Sigma-Aldrich, St. Louis, MO, USA). cDNA was prepared in 20 μL reactions using the iScriptTM cDNA Synthesis Kit according to manufacturer's instructions (Bio-Rad, Hercules, CA, USA). cDNA was diluted 5 times in nuclease-free water post synthesis. RT-qPCR experiments were run in duplicate reactions of 10 μL each containing 0.125 μL forward primer (10 pmol/μL), 0.125 μL reverse primer (10 pmol/μL), 3.750 μL nuclease-free water, 5 μL SYBR green (Roche, Bassel, Switzerland) and 1 μL cDNA. qPCR was performed on a Roche Lightcycler 480 with the following settings: heating at 95 °C for 15 min, 45 cycles of PCR (95 °C 10 s, 58 °C 20 s, 72 °C 15 s) and final elongation at 72 °C for 1 min. Normalization to *β-Actin* (*ACTB*) mRNA expression was performed using the X0 method [33]. Primer sequences are available in supplementary table 1.

2.4. Western blotting

For western blot analysis 50 μg protein extract was loaded on a Mini-protean TGX 4–15% gel (Bio-Rad). The gel was blotted onto an Amersham Hybond-P membrane (GE Healthcare). The membrane was blocked in 5% skimmed milk for 1 h and subsequently in 5% BSA for 1 h. The membrane was incubated with primary antibody diluted in 5% BSA blocking buffer and incubated over night at 4 °C. After washing the membrane was incubated with secondary antibody for 1 h. After washing, the membrane was processed with BM Chemiluminescence Blotting Substrate (Roche) and visualized using the ImageQuant LAS 4000 system (GE Healthcare). For western blot we used the following antibodies: Primary anti-ZEB1 (1:500, mouse, Nordic BioSite A301-922 A), anti-FGFR1 (1:500, rabbit, Cell Signaling Technology 9740S), anti-β-Actin (1:10000, rabbit, Sigma A2103), and secondary anti-rabbit (1:10000, goat, DAKO P0448) and anti-mouse (1:10000, goat, DAKO P0447).

2.5. Immunofluorescence

For immunofluorescence experiments cells were grown in 12 well plates on coverslips (VWR) pre-coated with poly-L-Lysine (Sigma) to a confluence of 60%. Cells were fixed in PBS containing 4% paraformaldehyde 20 min at room temperature and subsequently quenched for 5 min by the addition of glycine (final concentration 1.25 M). Cells were washed twice in cold PBS and permeabilized for 15 min on ice in PBS containing 0.5% Triton X-100 and protease inhibitors. The cells were blocked in 1% bovine serum albumin for 1 h and incubated with primary antibody dissolved in blocking buffer for 1 h at room temperature. Cell nuclei were stained with DAPI (Sigma-Aldrich) and mounted with Prolong Gold (Invitrogen, Thermo Fisher Scientific). For immunofluorescence were used antibodies anti-vimentin (1:500, mouse, Abcam AB20346), anti-E-cadherin (1:250, mouse, BD Biosciences 610182) and secondary Alexa 488 conjugated donkey anti-mouse IgG 1:2000 (Invitrogen, Thermo Fisher Scientific).

2.6. In silico expression analysis

The portal GenomicScape (http://www.genomicscape.com/) was used to analyze the cancer cell line encyclopedia (CCLE) lung non-small cell (lung_NSC) expression data and to calculate Spearman correlation

coefficients for candidate genes based on deposited microarray data from robust multi-array average (RMA) normalized Affymetrix Human Genome U133 Plus 2.0 Arrays. The cancer genome atlas (TCGA) expression data for lung adenocarcinoma (LUAD) tumors were analyzed using the cBioPortal (http://www.cbioportal.org/). Spearman expression correlation coefficients for candidate genes were calculated in cBioPortal using TCGA LUAD RNA sequencing expression data (V2 RNA-sequencing by expectation-maximization (RSEM)) in Z-score format.

2.7. Statistics

All statistic results for gene expression were calculated using repeated measures from independent experiments in form of biological triplicates. Data management and interpretations was performed using Excel and Graphpad Prism 6 software. Comparison of statistical significance was performed using unpaired Students t-tests and with a two-sided P value < 0.05 considered statistically significant. Expression correlation with a Spearman correlation coefficient $r < -0.25$ (negative correlation) or $r > 0.25$ (positive correlation) and two-tailed $P < 0.05$ was considered statistical significant.

3. Results and discussion

3.1. Increased FGFR1 expression is associated with EMT and concomitant ZEB1 expression in NSCLC

Using RNA expression data available for 114 NSCLC cell lines in the CCLE dataset lung_NSC, we determined the mRNA expression correlation between *FGFR1* and gene sets representing either fibroblast growth factor (FGF) signaling or an EMT signature (Fig. 1A). The FGF signaling gene set included *FGF2*, *FGFR2*, *FGFR3, FGFR4*, and *FGFRL1* (Fig. 1A). The EMT signature gene set included a previously published gene set including 16 marker genes for EMT in NSCLC [34], the EMT-TF genes *TWIST2*, *TCF3*, *TCF4*, *ZEB1*, and *ZEB2* [35], The EMT mRNA splice factor genes *ESRP1*, *ESRP2*, and *RBFOX2* [36], and the *EPCAM* gene encoding a well-established epithelial marker [37]. *FGFR1* showed pronounced correlation (Spearman correlation coefficient r = 0.59) to *FGF2* expression, which is in line with the demonstrated FGFR1-FGF2 signaling loop in NSCLC [20,26], whereas *FGFR2* and *FGFR3* expression negatively correlated with *FGFR1* expression (r = −0.30 and r = –0.28, respectively). This is in accordance with a previous comprehensive study by Gröger et al., who identified genes systematically differently expressed as a result of EMT at various cellular backgrounds and identified *FGFR1* expression to be increased and *FGFR2* and *FGFR3* expression to be decreased [38]. For the EMT signature gene set, we observed a negative correlation ($r < -0.25$) between *FGFR1* and the epithelial markers *CDH1 (*encoding E-cadherin*)*, *DSP, EPCAM, ITGB6, ESRP1,* and *ESRP2*, and a positive correlation ($r > 0.25$) between *FGFR1* and the mesenchymal markers *CDH2*, *MMP2*, and *VIM* (encoding Vimentin*)*. In addition, we observed a pronounced positive expression correlation between *FGFR1* and *ZEB1* (r = 0.6) and *ZEB2* (r = 0.49), whereas mRNA for other EMT-TFs displayed from minor (*TWIST1* and *TCF4* with r = 0.29 and r = 0.26, respectively) to no expression correlation ($-0.25 < r < 0.25$) (Fig. 1A). Expression correlation between *FGFR1* and *ZEB1* mRNA was also identified in a previous study examining 38 NSCLC cell lines [39]. In the dataset NSCLC LUAD from TCGA, we observed an overall similar mRNA expression correlation pattern between *FGFR1* and *FGF* signaling genes, as well as between *FGFR1* and EMT signature genes including *ZEB1* (r = 0.5) (Fig. S1A). We further focused on the expression correlation between *FGFR1* and *ZEB1*. We questioned how the gene sets presented in Fig. 1A expression correlated with *ZEB1*. In the dataset CCLE lung_NSC, as well as in the dataset TCGA LUAD, the *ZEB1* expression correlation pattern resembled the pattern observed for *FGFR1* (Fig. 1B and Fig. S1B). This further supports *ZEB1* and *FGFR1* expression being associated with the same FGF signaling and EMT signature profile in NSCLC. Expression correlation plots for *FGFR1* and *ZEB1* revealed, despite overall correlation, the presence of NSCLC cell lines and LUAD tumors with concomitant relatively high *FGFR1* and low *ZEB1* expression, whereas the opposite scenario was less evident (Fig. 1C and Fig. S1C). Analyses of available CCLE lung_NSC IC50 data showed that *FGFR1*, *FGF2* and *ZEB1* expression was positively correlated with IC50 for the EGFR-TKI erlotinib, whereas *EGFR* expression and erlotinib IC50 negatively correlated (Fig. S2A). No correlation was evident between *EGFR* and *FGFR1*, *FGF2* and *ZEB1* expression in the dataset CCLE lung_NSC (Fig. S2A). In the dataset TCGA LUAD, *FGFR1*, *FGF2* and *ZEB1* expression was not correlated to either survival or *EGFR* expression (Fig. S2C).

We then questioned whether the *ZEB1* and *FGFR1* expression correlation was also present in the subset of CCLE lung_NSC cell lines and TCGA LUAD tumors presented with activating *EGFR*-mutations. In the eight CCLE lung_NSC cell lines as well as in the 18 LUAD tumor samples harboring activating *EGFR* mutations, positive Spearman correlation coefficients for *ZEB1* and *FGFR1* expression were present (Fig. 1C and Fig. S1C). However, it should be noted that a clear limitation of this specific analysis is the presence of few *EGFR*-mutated samples, and the expression correlation result is accordingly not formally significant for the CCLE lung_NSC samples (Fig. 1C). In *EGFR*-mutated CCLE lung_NSC cell lines, positive correlation of *FGFR1*, *FGF2* and *ZEB1* expression with erlotinib IC50, negative correlation of *EGFR* expression with erlotinib IC50, and inverse correlation of *EGFR* with *FGFR1*, *FGF2* and *ZEB1* expression, were indicated but again not formally significant (Fig. S2B). Such correlation patterns are in alignment with previous results showing EMT and FGFR1-FGF2 expression being involved in intrinsic and acquired resistance to EGFR-TKI treatment in *EGFR*-mutated NSCLC cells [16–21,25–27]. In the dataset TCGA LUAD, *FGFR1*, *FGF2* and *ZEB1* expression was not systematically correlated to either survival or *EGFR* expression in the subset of samples with activating *EGFR*-mutations (Fig. S2D).

3.2. ZEB1-associated EMT results in increased FGFR1 expression in NSCLC cells

The *in silico* analyses using datasets CCLE lung_NSC and TCGA LUAD indicated that *ZEB1*-associated EMT correlates with *FGFR1* expression. This was experimentally supported using our previously described EGFR-TKI resistance-based EMT model in the HCC827 NSCLC cell line, harboring the activating *EGFR*-mutation exon19del E746–A750 [17]. Briefly described, this EMT model was established by treating epithelial HCC827 cells with an escalating dose of erlotinib until resistance was acquired at 5μM erlotinib [17]. From the HCC827 erlotinib resistant (ER) cell population, individual cell clones were isolated and HCC827 ER cell clones 4, 7, and 10 were characterized to be EMT-induced given that immunofluorescence analyses showed increased Vimentin expression and decreased E-cadherin expression relative to the parental HCC827 cell line [17]. This was further supported by RT-qPCR analyses [17]. In line with these observations and the *in silico* analyses described above, we observed in such HCC827 ER cell clones increased *ZEB1* expression and either small or no significant expression changes for *TWIST1*, *SNAI1* (also called *SNAIL*) and *SNAI2* (also called *SLUG*) (Fig. 1D). An increase in *ZEB2* expression in the HCC827 ER cell clones was not statistically significant (Fig. 1D). This was most likely owed to a very low and variable *ZEB2* expression both in the parental HCC827 cell line and HCC827 ER cell clones. Importantly, *FGFR1* expression was increased approximately 15-fold in the HCC827 ER cell clones relative to the parental HCC827 cell line (Fig. 1D). We note that the 15-fold increased *FGFR1* expression in the HCC827 ER cell clones is accompanied with acquired sensitivity for FGFR1 inhibition with AZD5447 supporting that FGFR1 signaling can be a bypass mechanism in EMT-induced EGFR TKI resistance [17,27]. Moreover, *VIM* expression was increased and *CDH1* and *ESRP1* expression decreased in HCC827 ER cell clones in accordance with transition to a mesenchymal phenotype

(Fig. 1D).

To investigate whether EMT drives a concomitant increase in *FGFR1* expression, or increased *FGFR1* expression drives *ZEB1*-associated EMT in the genetic background of an *EGFR*-activating mutation, we first addressed the former scenario. This was done by inducing EMT in the two NSCLC cell lines PC9 and HCC827 with the former also harboring the activating *EGFR*-mutation exon19del E746–A750. The cell lines were treated with the StemXvivo EMT-inducing media supplement composed of a multitude of antibodies and cytokines, *e.g.*, Wnt-5a and TGF-β1 cytokines, and E-cadherin, sFRP-1, and Dkk-1 antibodies (materials and methods). This approach to induce EMT was chosen to obtain a final EMT profile not restricted to commandeering from a single EMT-inducing pathway. Untreated HCC827 and PC9 cells formed a tight conformation with E-cadherin staining localized to the membranes of cell-cell contacts (Fig. 1E). After StemXvivo treatment, HCC827 cells adapted a more spindle-shape morphology with more diffuse E-

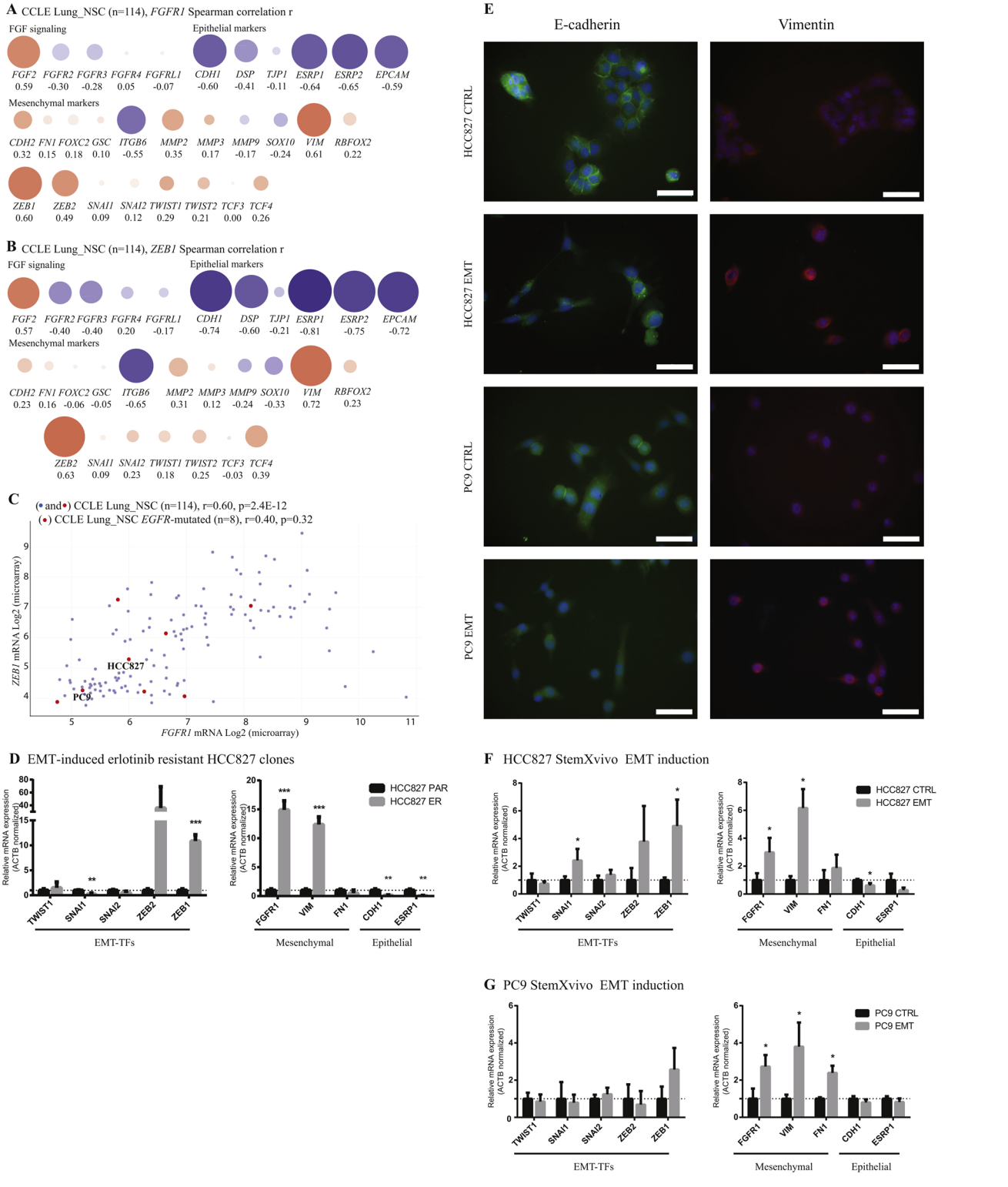

(caption on next page)

Fig. 1. *FGFR1* and *ZEB1* expression in EMT. A–B) mRNA expression correlation analysis between *FGFR1* (panel A) or *ZEB1* (panel B) and gene sets representing FGF signaling and an EMT signature using available mRNA expression data from the CCLE dataset lung_NSC (n = 114). Spearman correlation coefficients and accompanying P values were calculated using Genomicscape. Spearman correlation coefficients are shown and in addition illustrated graphical in proportions using red and blue to symbolize positive and negative correlation, respectively. Spearman correlation coefficients r < -0.25 (negative correlation) and r > 0.25 (positive correlation) were all having P < 0.01. C) mRNA expression correlation analysis for *FGFR1* and *ZEB1* mRNA in the CCLE dataset lung_NSC (n = 114). Correlation coefficients and accompanying P values were calculated using Genomicscape. Red dots indicate lung_NSC cell lines with activating *EGFR*-mutations (n = 8). The *EGFR*-mutated cell lines HCC827 and PC9 cell lines are annotated. D) RT-qPCR analysis of mRNA expression for EMT markers and EMT-TFs in parental and EMT-induced HCC827 ER cell clones. Expression levels were normalized to *ACTB* and subsequently to the expression in parental HCC827 cells. E) Immunofluorescence staining of EMT markers E-cadherin (green, epithelial marker) and Vimentin (red, mesenchymal marker) in HCC827 and PC9 cells treated with or without StemXvivo EMT inducing reagent (40X, scale bar 50 μm). F–G) RT-qPCR analysis of mRNA expression for EMT markers and EMT-TFs in HCC827 (F) and PC9 (G) cells treated with or without StemXvivo EMT inducing reagent. Expression levels were normalized to *ACTB* and subsequently to the expression in respective control cells. Statistical significance was determined by an unpaired Students *t*-test and illustrated as * P < 0.05; ** P < 0.01; *** P < 0.001; **** P < 0.0001 (For interpretation of the references to colour in this figure legend, the reader is referred to the web version of this article.).

cadherin staining (Fig. 1E). In addition, Vimentin staining was more intense (Fig. 1E). In PC9 cells, an EMT phenotypic shift following StemXvivo treatment was not pronounced, but we noticed more intense Vimentin staining (Fig. 1E). RT-qPCR analysis verified EMT characteristics to be present in HCC827 cells following StemXvivo treatment, as evidenced by a significant increase in mRNA expression for the mesenchymal marker *VIM* and decreased expression of the epithelial marker *CDH1* (Fig. 1F). Moreover, mRNA expression for *ZEB1* and *SNAI1* was increased, whereas the mRNA expression of other EMT-TFs did not significantly change (Fig. 1F). Importantly, the induction of EMT in HCC827 cells was accompanied by a 3-fold increase in *FGFR1* expression (Fig. 1F). This increase was modest compared to the increase in *FGFR1* expression in the EMT-induced HCC827 ER cell clones (Fig. 1D and F) but supports that EMT-induction by StemXvivo mediates an increase in *FGFR1* expression in HCC827 cells. We find it questionable if the 3-fold increase in *FGFR1* expression following StemXvivo EMT-induction is sufficient to mediate a measurable change in EGFR-TKI sensitivity in these cells. We note that we previously showed that a 50-fold increase in *FGFR1* expression in the HCC827 cell line had an effect for intrinsic erlotinib-sensitivity [27]. Moreover, a possible StemXvivo-mediated change in EGFR-TKI sensitivity in the HCC827 cells could be mediated by other EMT-associated processes than FGFR1-mediated bypass signaling [9]. In PC9 cells, no significant mRNA expression changes for EMT-TFs were observed following StemXvivo supplement (Fig. 1G). An increase in *ZEB1* expression was nearly significant but a large variation in actual fold change was observed between the biological replicates (Fig. 1G). We note that PC9 cells have a lower basal expression of *ZEB1* and *ZEB2* compared to HCC827 cells (data not shown and Fig. 1C). Low expression could explain the high variability in RT-qPCR experiments and non-significant results concerning *ZEB1* expression in PC9 cells. In addition, this suggests a stronger epithelial phenotype in PC9 cells than in HCC827 cells. This could explain the inefficient EMT induction by StemXvivo in PC9 cells, in the sense that a stronger stimuli would be needed to mediate EMT due to the stronger epithelial polarization. This is further supported by the observation that PC9 cells are unresponsive to TGF-β induced EMT [40]. Note that TGF-β is a main component of the StemXvivo reagent. However, StemXvivo treatment in PC9 cells resulted in a 3-fold increase in *FGFR1* expression (Fig. 1G). *Vim* and *FN1* expression were also increased (Fig. 1G). Collectively the StemXvivo results in HCC827 and PC9 cell lines indicates that EMT-induction drives increased *FGFR1* expression in *EGFR*-mutated NSCLC cells.

We next investigated the effect of increased *ZEB1* expression for EMT and *FGFR1* expression in *EGFR*-mutated NSCLC cells. We focused on the EMT-TF ZEB1 owing to the following observations: i) The observed positive expression correlation between *ZEB1* and *FGFR1* in the NSCLC datasets (Fig. 1) [39]; ii) The concomitant increase in *ZEB1* and *FGFR1* expression following StemXvivo-mediated EMT-induction (Fig. 1), iii) The association between increased *ZEB1* expression and EMT [9,35,41–46], and iv) The association between increased *FGFR1* expression and EMT in acquired EGFR-TKI resistance in NSCLC [17,20]. We increased expression of the endogenous *ZEB1* gene in PC9 and HCC827 cell lines utilizing the CRISPR-dCas9-SAM approach [31]. Three gRNAs complementary to the *ZEB1* promoter were assembled into a single a vector and used for stable transfection of PC9 and HCC827 cells beforehand transduced to express dCas9-vp64 and MS2-p65-HIF-1 [27]. By this approach, the cell lines PC9^{gZEB1} and HCC827^{gZEB1} were generated. In parallel, gRNA designed to target the mCherry fluorescent protein gene (gCTR) was used to establish control cell lines PC9^{gCTR} and HCC827^{gCTR}. RT-qPCR analysis revealed a 30-fold increase in *ZEB1* expression in PC9^{gZEB1} cells and a 6-fold increase in *ZEB1* expression in HCC827^{gZEB1} cells (Fig. 2A). Notably, parental HCC827 and HCC827^{gCTR} cells displayed *ZEB1* expression to a higher level than in the parental PC9 and PC9^{gCTR} cells, whereas the *ZEB1* expression level was similar in PC9^{gZEB1} and HCC827^{gZEB1} cells. Western blot analysis revealed an increase in ZEB1 protein in PC9^{gZEB1} and HCC827^{gZEB1} cells relative to the respective control cell lines (Fig. 2B). This indicated that the described miRNA-mediated inhibition of *ZEB1* mRNA translation could be circumvented to allow increased ZEB1 protein production (Fig. 2B) [47]. In HCC827^{gZEB1} cells, EMT phenotype characteristics were only evidenced by decreased *CDH1* expression and increased *ZEB2* expression (Fig. 2A). This indicated that the level of ZEB1 expression in the HCC827^{gZEB1} cells was not sufficient to further drive a pleiotropy of EMT characteristics. We note an insignificant increase in *FGFR1* mRNA expression (2-fold) in HCC827^{gZEB1} cells (Fig. 2A). Western blot analysis indicated increased FGFR1 protein levels in HCC827^{gZEB1} cells compared to HCC827^{gCTR} cells (Fig. 2B). In PC9^{gZEB1} cells, more indications of EMT were observed with increased expression of *VIM* and decreased expression of *ESRP1* and *CDH1* (Fig. 2A). Moreover, we observed a minor increase in *SNAI2* expression and note an insignificant increase (20-fold) in *ZEB2* expression (Fig. 2A). For the latter, the lack of significance was attributed to the increased *ZEB2* expression varied from few-fold to 50-fold activation among the three biological replicates examined. Immunostaining for E-cadherin and Vimentin supported the EMT phenotype in PC9^{gZEB1} cells (Fig. 2C). *FGFR1* expression was increased (4-fold) in PC9^{gZEB1} compared to PC9^{gCTR} (Fig. 2A). Western blot analysis supported the mRNA expression data by showing an increased FGFR1 protein expression level in PC9^{gZEB1} cells compared to PC9^{gCTR} cells (Fig. 2C). The results show that increasing the expression of the EMT-TF ZEB1, at least in the PC9^{gZEB1} NSCLC cell model, drives EMT and an accompanied increase in *FGFR1* expression. The higher basal expression of *ZEB1* in HCC827 cells compared to PC9 cells further supports that PC9 cells are more epithelial than HCC827 cells. Thus, despite we observed more pronounced EMT related expression changes in PC9^{gZEB1} compared to HCC827^{gZEB1}, the endpoint mesenchymal phenotypes were comparable. To the best of our knowledge, ZEB1 has not been identified directly involved in transcriptional regulation of the *FGFR1* gene and our results showing that *ZEB1* induction results in increased *FGFR1* expression could be a consequence of either direct or indirect regulation. Future experiments wherein ZEB1 is depleted either transiently or genetically will be important to delineate if ZEB1 is a direct regulator of *FGFR1* expression or the increase in *FGFR1* expression is an indirect consequence of ZEB1 induced EMT.

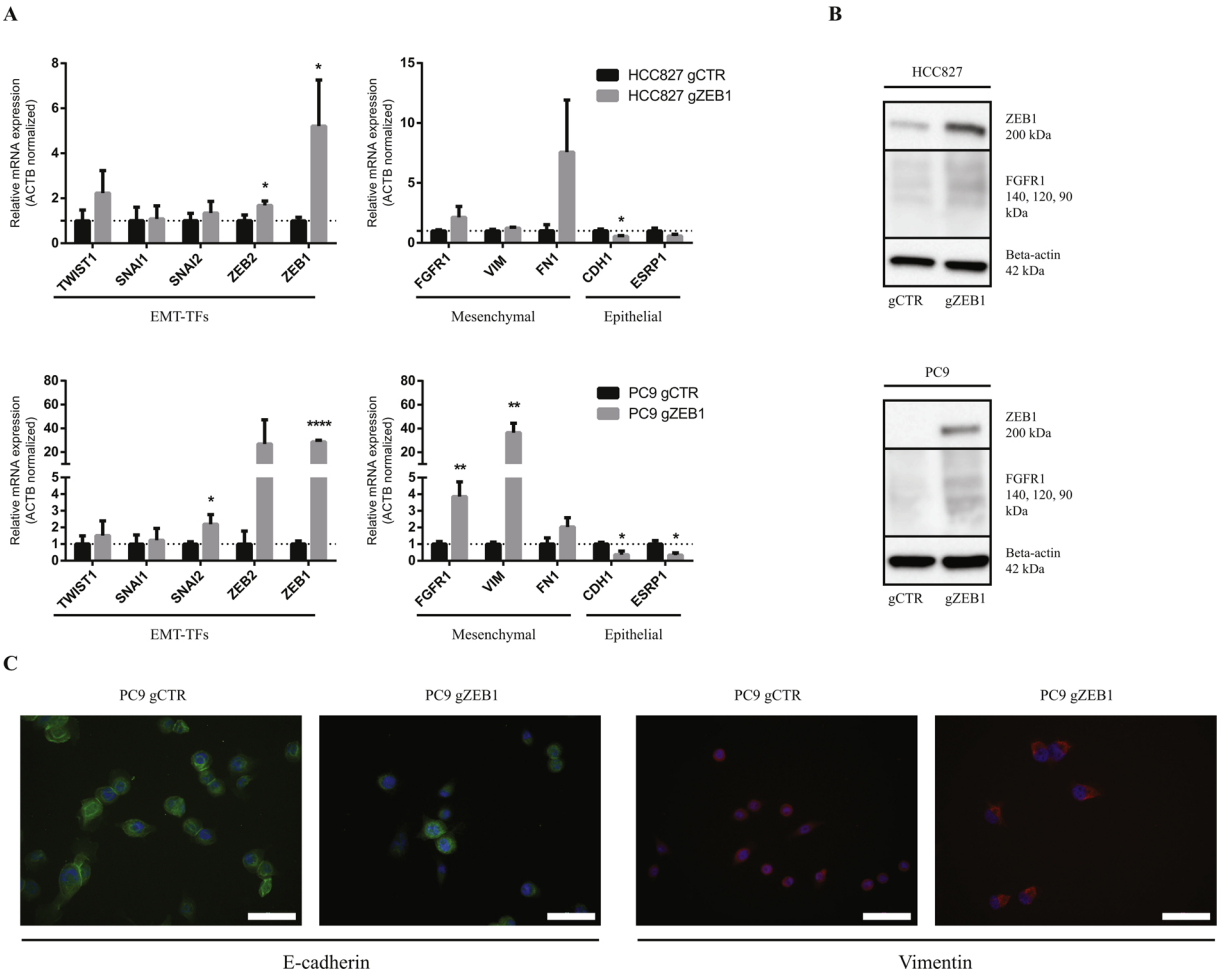

Fig. 2. CRISPR-dCAS9-SAM-mediated induction of endogenous *ZEB1* expression. A) RT-qPCR analysis of mRNA expression for EMT markers and EMT-TFs in HCC827 (top) and PC9 (bottom) cells with CRISPR-dCAS9-SAM and either non-targeting gRNA control (gCTR) or *ZEB1* activating gRNAs (gZEB1). Expression levels were normalized to *ACTB* and subsequently to the expression in gCTR cells. Statistical significance was determined by an unpaired Students *t*-test and illustrated as * $P < 0.05$; ** $P < 0.01$; *** $P < 0.001$; **** $P < 0.0001$. B) Western blot analysis. 50 µg protein lysate was used for western blot analysis of ZEB1, FGFR1, and β-Actin. C) Immunofluorescence staining of EMT markers E-cadherin (green, epithelial marker) and Vimentin (red, mesenchymal marker) in PC9 cells (40X, scale bar 50 µm) (For interpretation of the references to colour in this figure legend, the reader is referred to the web version of this article.).

3.3. Increased FGFR1 expression does not induce EMT in NSCLC cells

We previously described that CRISPR-dCas9-SAM mediated 50-fold induction of endogenous *FGFR1* which resulted in intrinsic resistance to the growth inhibiting effect of EGFR-TKIs in PC9 and HCC827 cells [27]. This showed the capability of increased *FGFR1* expression to sustain bypass signaling when EGFR-mediated signaling is blocked, but whether EMT was concomitant was not addressed [27]. To determine if an increase in *FGFR1* expression is sufficient to drive EMT in *EGFR*-mutated NSCLC cells, we used CRISPR-dCas9-SAM to induce endogenous *FGFR1* expression in PC9^{gFGFR1} and HCC827^{gFGFR1} cells [27]. RT-qPCR revealed a 50-fold increase in *FGFR1* mRNA expression in PC9^{gFGFR1} cells and HCC827^{gFGFR1} cells, and in accordance, western blot analysis showed an increase in FGFR1 protein in PC9^{gFGFR1} cells and HCC827^{gFGFR1} cells (Fig. 3A and B) [27]. In RT-qPCR analyses of the HCC827^{gFGFR1} cells we did not observe mRNA expression changes for EMT-TFs or other EMT marker genes (Fig. 3A). Thus, the increased *FGFR1* expression in HCC827^{gFGFR1} cells is not mediating EMT-induction. RT-qPCR analyses of PC9^{gFGFR1} cells did not reveal expression changes for EMT-TFs (Fig. 3A). In PC9^{gFGFR1} cells we observed decreased *VIM* and increased *CDH1* expression indicating a more epithelial-like phenotype adapted by the PC9^{gFGFR1} cells (Fig. 3A). On top of this, we did not observe gene expression changes indicative of EMT following stimulation of PC9^{gCTR} cells and PC9^{gFGFR1} cells as well as HCC827^{gCTR} cells and HCC827^{gFGFR1} cells with 20 ng/mL FGF2 for 48 h (Fig. S3). Lastly, to determine if EMT occurred in a minor population of the PC9^{gFGFR1} and HCC827^{gFGFR1} cells, we performed E-cadherin and Vimentin immunostainings (Fig. S4). We were unable to identify cell subpopulations with an EMT phenotype in PC9^{gFGFR1} and HCC827^{gFGFR1} cells, and stimulation with FGF2 had no detectable consequence in this regard (Fig. S4). We conclude that increased *FGFR1* expression *per se* is not sufficient to drive gene expression changes associated with EMT in HCC827 and PC9 cells.

3.4. FGFR1 mRNA isoform expression following EMT

FGFR1, *FGFR2*, and *FGFR3* genes produce different mRNA isoforms through alternative splicing (Fig. 4A) [22,48]. The alternative splicing of mutually exclusive exons 8 and 9, corresponding to the Ig III loop, generates the IIIb and IIIc isoforms mainly expressed in epithelial and mesenchymal tissues, respectively [49,50]. IIIc protein has increased FGF2 binding affinity, whereas IIIb protein preferentially binds FGF7 and FGF10 [51]. Isoform switching in FGFR2 due to this alternative splicing is able to drive EMT as well as cancer progression in some cellular backgrounds [52–54]. *FGFR1 IIb* and *FGFR1 IIIc* are both expressed in NSCLC samples, with *FGFR1 IIIc* being less expressed in epithelial cell types [55]. To examine *FGFR1* mRNA isoform expression in PC9 and HCC827 cells, we designed RT-qPCR primers for detecting

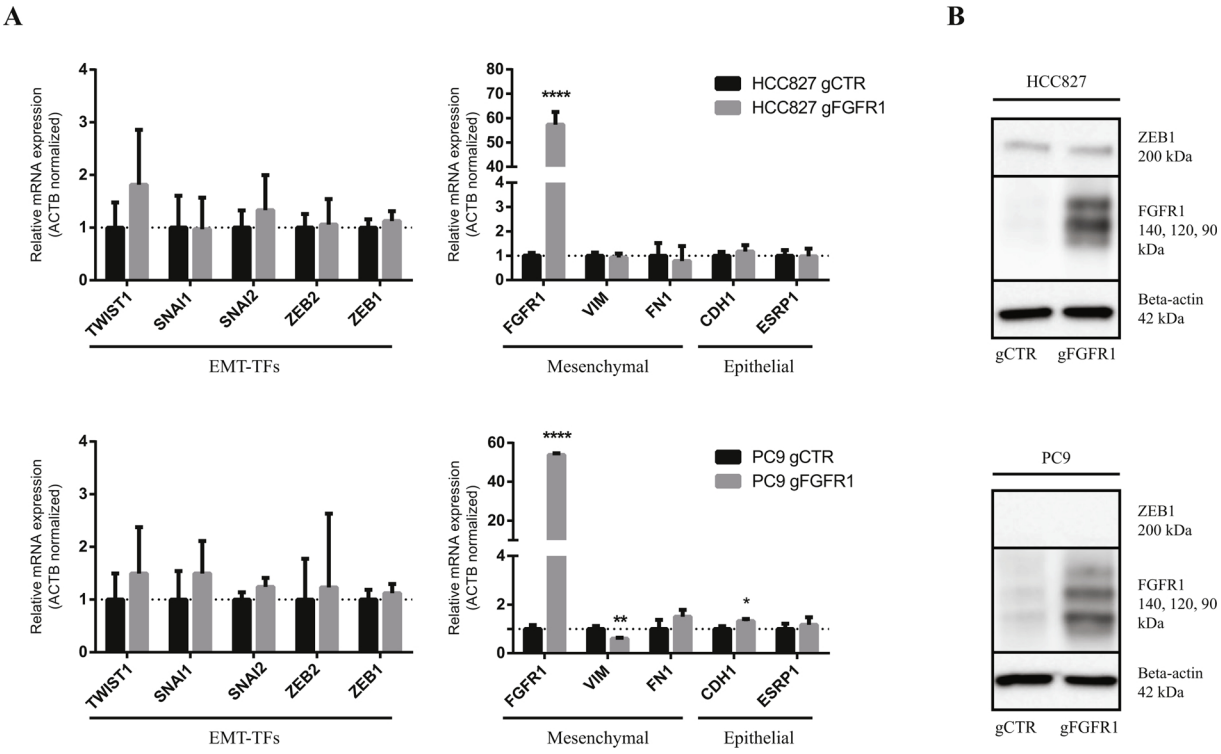

Fig. 3. CRISPR-dCAS9-SAM-mediated induction of endogenous *FGFR1* expression. A) RT-qPCR analysis of mRNA expression for EMT markers and EMT-TFs in HCC827 (top) and PC9 (bottom) cells with CRISPR-dCAS9-SAM and either non-targeting gRNA control (gCTR) or *FGFR1* activating gRNAs (gFGFR1). Expression levels were normalized to *ACTB* and subsequently to the expression of gCTR cells. Statistical significance was determined by an unpaired Students *t*-test and illustrated as * $P < 0.05$; ** $P < 0.01$; *** $P < 0.001$; **** $P < 0.0001$. B) Western blot analysis. 50 µg protein lysate was used for western blot analysis of ZEB1, FGFR1, and β-Actin.

FGFR1 exon 8 inclusion (*FGFR1 IIIb*) or exon 9 inclusion (*FGFR1 IIIc*) (Fig. 4A). In line with previous observations for FGFR2 [52–54], in the EMT-induced HCC827 ER cell clones, *FGFR1 IIIc* was relative more expressed than *FGFR1 IIIb* (Fig. 4B). This represents a proof-of-principle for the expected preferential increase in *FGFR1 IIIc* isoform expression following EMT in *EGFR*-mutated NSCLC cells. StemXvivo-supplemented HCC827 cells revealed an increase of both *FGFR1 IIIb* and *FGFR1 IIIc* isoforms, but the increase for the latter most pronounced (Fig. 4C). In PC9 cells, neither *FGFR1 IIIb* nor *FGFR1 IIIc* expression significantly changed following StemXvivo treatment. We note that in this PC9 StemXvivo EMT cell model we only have observed modest indications of EMT (Fig. 1). CRISPR-dCas9-SAM mediated *ZEB1* induction in HCC827^{gZEB1} cells resulted in increased *FGFR1-IIIb* expression, whereas increased *FGFR1 IIIc* expression was not significant (Fig. 4C). We note that in the HCC827^{gZEB1} EMT cell model we only observed modest indications of EMT and an insignificant increase in *FGFR1* expression (Fig. 2). In PC9^{gZEB1} cells, which have EMT characteristics (Fig. 2), we note an insignificant increase in *FGFR1 IIIc* expression, whereas *FGFR1 IIIb* expression was similar to the expression in the control cells PC9^{gCTR} (Fig. 4C). Summarized, cells with the strongest EMT characteristics, namely HCC827 ER, HCC827 StemXvivo, and PC9^{gZEB1}, showed a change in *FGFR1* isoform stoichiometric towards *FGFR1 IIIc* expression. Examining CRISPR-dCas9-SAM mediated *FGFR1* induction showed that *FGFR1 IIIb* and *FGFR1 IIIc* expression concordantly increased in PC9^{gFGFR1} cells relative to PC9^{gCTR} cells and in HCC827^{gFGFR1} cells relative to HCC827^{gCTR} cells (Fig. 4B). Since both *FGFR1* isoforms have increased expression following CRISPR-dCas9-SAM-mediated induction of endogenous *FGFR1*, the absence of concomitant EMT is most likely not a consequence of lacking the FGFR1 IIIc isoform. However, we cannot exclude the possibility that a change in the balance in *FGFR1* isoforms in consequence of altered splice factor regulation initially in the EMT process could take part in an EMT promoting regulatory loop in NSCLC cells. We note decreased expression of the epithelial cell specific splice factors ESRP1 and ESRP2 during EMT and this could be one candidate mechanism to mediate a change in *FGFR1 IIIb* and *IIIc* isoform balance [56,57].

4. Conclusion

From the presented analyses, we conclude that in *EGFR*-mutated NSCLC cell lines, ZEB1 is a driver of EMT and a concomitant increase in *FGFR1* expression, whereas *FGFR1* expression can be increased without driving concomitant EMT. A limitation of the described study is the usage of only the NSCLC cell lines PC9 and HCC827 in the analyses. Therefore, whether the cause-and-effect conclusion is valid beyond the genetic background of these analyzed cell lines still needs verification. FGFR1 signaling is reported to provide both intrinsic and EMT-associated acquired resistance in consequence of TKI treatment of *EGFR*-mutated NSCLC cells [17,20,25–27,58]. The latter is in line with the observation of FGFR1 being a RTK relatively systematically having increased expression along with EMT [38]. The consensus is that activation of the auto-regulatory FGFR1 and FGF2 loop provides a bypass signaling mechanism to the pharmacological-inhibited EGFR signaling pathway [20,26]. Our findings concerning cause-and-effect relationship between *ZEB1*-associated EMT and *FGFR1* expression indicates a model in which acquired EGFR-TKI resistance in *EGFR*-mutated NSCLC cells can be the result of increased *FGFR1* expression in consequence of the EMT process, whereas intrinsic EGFR-TKI resistance can be the result of an EMT-independent increase in *FGFR1* expression. The common outcome will be the observed FGFR1-mediated bypass signaling allowing growth of *EGFR*-mutated NSCLC cells despite TKI-mediated blocking of active EGFR-signaling [17,20,25,27].

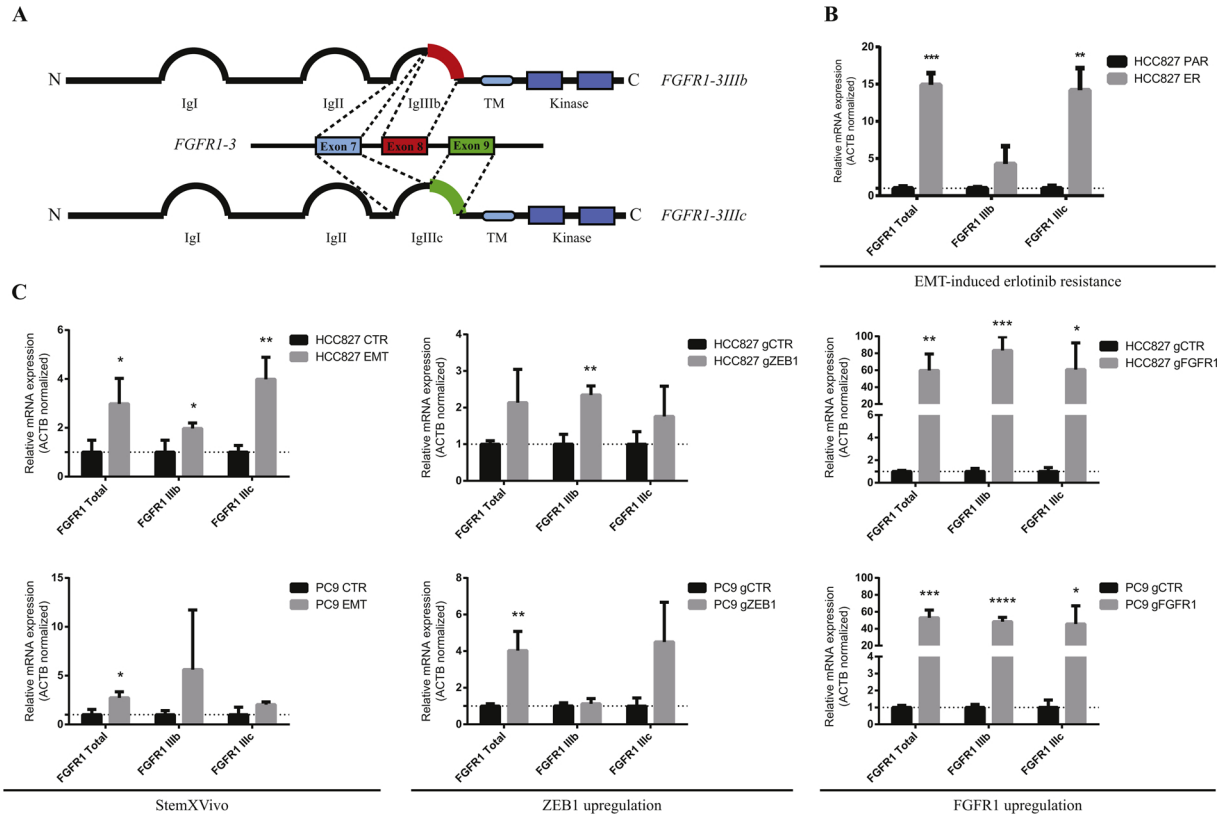

Fig. 4. *FGFR1* mRNA isoform expression analysis. A) Illustration of alternative splicing in *FGFR1*, *FGFR2*, and *FGFR3* involving the mutually exclusive exons 8 and 9. Inclusion of exon 8 encodes the isoform with the IIIb loop primarily expressed in epithelial cells whereas inclusion of exon 9 encodes the isoform with the IIIc loop primarily expressed in mesenchymal cells. Illustration is modified from [47]. B) RT-qPCR analysis of mRNA expression of *FGFR1* isoforms in parental HCC827 cells and EMT-induced HCC827 ER cell clones. Expression levels were normalized to *ACTB* and subsequently to the expression in parental HCC827 cells. C) RT-qPCR analysis of mRNA expression of *FGFR1* isoforms in HCC827 (top) and PC9 (bottom) cells treated or untreated with StemXvivo EMT-inducing reagent (left panels), with CRISPR-dCAS9-SAM-mediated *ZEB1* induction or corresponding control cells (central panels), and with CRISPR-dCAS9-SAM-mediated *FGFR1* induction or corresponding control cells (right panels). Expression levels were normalized to *ACTB* and subsequently to the expression in respective control cells. Statistical significance was determined by an unpaired Students *t*-test and illustrated as * $P < 0.05$; ** $P < 0.01$; *** $P < 0.001$; **** $P < 0.0001$.

Conflict of interest

The authors declare no conflict of interest.

Funding

This study was supported by Dagmar Marshalls Mindelegat, Fabrikant Einar Willumsens Mindelegat, Marie og Børge Kroghs Fond, P. A. Messerschmidt og Hustrus Fond, Thora og Viggo Grove´s Mindelegat, and Familien Erichsens Familiefond.

Acknowledgement

JVN and KRG were supported by PHD fellowships from Health, Aarhus University, Denmark.

Appendix A. Supplementary data

Supplementary material related to this article can be found, in the online version, at doi:https://doi.org/10.1016/j.lungcan.2019.04.023.

References

[1] R.L. Siegel, K.D. Miller, A. Jemal, Cancer statistics, 2016, CA Cancer J. Clin. 66 (1) (2016) 7–30.
[2] C. Gridelli, A. Rossi, D.P. Carbone, J. Guarize, N. Karachaliou, T. Mok, F. Petrella, L. Spaggiari, R. Rosell, Non-small-cell lung cancer, Nat. Rev. Dis. Primers 1 (2015) 15009.
[3] L.V. Sequist, V.A. Joshi, P.A. Janne, A. Muzikansky, P. Fidias, M. Meyerson, D.A. Haber, R. Kucherlapati, B.E. Johnson, T.J. Lynch, Response to treatment and survival of patients with non-small cell lung cancer undergoing somatic EGFR mutation testing, Oncologist 12 (1) (2007) 90–98.
[4] J.A. Engelman, P.A. Janne, Mechanisms of acquired resistance to epidermal growth factor receptor tyrosine kinase inhibitors in non-small cell lung cancer, Clin. Cancer Res. 14 (10) (2008) 2895–2899.
[5] T.J. Lynch, D.W. Bell, R. Sordella, S. Gurubhagavatula, R.A. Okimoto, B.W. Brannigan, P.L. Harris, S.M. Haserlat, J.G. Supko, F.G. Haluska, D.N. Louis, D.C. Christiani, J. Settleman, D.A. Haber, Activating mutations in the epidermal growth factor receptor underlying responsiveness of non-small-cell lung cancer to gefitinib, N. Engl. J. Med. 350 (21) (2004) 2129–2139.
[6] J.G. Paez, P.A. Janne, J.C. Lee, S. Tracy, H. Greulich, S. Gabriel, P. Herman, F.J. Kaye, N. Lindeman, T.J. Boggon, K. Naoki, H. Sasaki, Y. Fujii, M.J. Eck, W.R. Sellers, B.E. Johnson, M. Meyerson, EGFR mutations in lung cancer: correlation with clinical response to gefitinib therapy, Science 304 (5676) (2004) 1497–1500.
[7] G. da Cunha Santos, F.A. Shepherd, M.S. Tsao, EGFR mutations and lung cancer, Annu. Rev. Pathol. 6 (2011) 49–69.
[8] L.V. Sequist, T.J. Lynch, EGFR tyrosine kinase inhibitors in lung cancer: an evolving story, Annu. Rev. Med. 59 (2008) 429–442.
[9] K.R. Jakobsen, C. Demuth, B.S. Sorensen, A.L. Nielsen, The role of epithelial to mesenchymal transition in resistance to epidermal growth factor receptor tyrosine kinase inhibitors in non-small cell lung cancer, Transl. Lung Cancer Res. 5 (2) (2016) 172–182.
[10] B. Du, J.S. Shim, Targeting epithelial-mesenchymal transition (EMT) to overcome drug resistance in cancer, Molecules 21 (7) (2016).
[11] M.A. Nieto, R.Y. Huang, R.A. Jackson, J.P. Thiery, Emt: 2016, Cell 166 (1) (2016) 21–45.
[12] B. De Craene, G. Berx, Regulatory networks defining EMT during cancer initiation and progression, Nat. Rev. Cancer 13 (2) (2013) 97–110.
[13] T. Arumugam, V. Ramachandran, K.F. Fournier, H. Wang, L. Marquis, J.L. Abbruzzese, G.E. Gallick, C.D. Logsdon, D.J. McConkey, W. Choi, Epithelial to mesenchymal transition contributes to drug resistance in pancreatic cancer, Cancer Res. 69 (14) (2009) 5820–5828.
[14] D.J. McConkey, W. Choi, L. Marquis, F. Martin, M.B. Williams, J. Shah, R. Svatek, A. Das, L. Adam, A. Kamat, A. Siefker-Radtke, C. Dinney, Role of epithelial-to-

mesenchymal transition (EMT) in drug sensitivity and metastasis in bladder cancer, Cancer Metastasis Rev. 28 (3-4) (2009) 335–344.
[15] J. Huang, H. Li, G. Ren, Epithelial-mesenchymal transition and drug resistance in breast cancer (Review), Int. J. Oncol. 47 (3) (2015) 840–848.
[16] S. Thomson, E. Buck, F. Petti, G. Griffin, E. Brown, N. Ramnarine, K.K. Iwata, N. Gibson, J.D. Haley, Epithelial to mesenchymal transition is a determinant of sensitivity of non-small-cell lung carcinoma cell lines and xenografts to epidermal growth factor receptor inhibition, Cancer Res. 65 (20) (2005) 9455–9462.
[17] K.R. Jakobsen, C. Demuth, A.T. Madsen, D. Hussmann, J. Vad-Nielsen, A.L. Nielsen, B.S. Sorensen, MET amplification and epithelial-to-mesenchymal transition exist as parallel resistance mechanisms in erlotinib-resistant, EGFR-mutated, NSCLC HCC827 cells, Oncogenesis 6 (4) (2017) e307.
[18] H. Uramoto, T. Iwata, T. Onitsuka, H. Shimokawa, T. Hanagiri, T. Oyama, Epithelial-mesenchymal transition in EGFR-TKI acquired resistant lung adenocarcinoma, Anticancer Res. 30 (7) (2010) 2513–2517.
[19] Y. Lin, X. Wang, H. Jin, EGFR-TKI resistance in NSCLC patients: mechanisms and strategies, Am. J. Cancer Res. 4 (5) (2014) 411–435.
[20] K.E. Ware, T.K. Hinz, E. Kleczko, K.R. Singleton, L.A. Marek, B.A. Helfrich, C.T. Cummings, D.K. Graham, D. Astling, A.C. Tan, L.E. Heasley, A mechanism of resistance to gefitinib mediated by cellular reprogramming and the acquisition of an FGF2-FGFR1 autocrine growth loop, Oncogenesis 2 (2013) e39.
[21] L.V. Sequist, B.A. Waltman, D. Dias-Santagata, S. Digumarthy, A.B. Turke, P. Fidias, K. Bergethon, A.T. Shaw, S. Gettinger, A.K. Cosper, S. Akhavanfard, R.S. Heist, J. Temel, J.G. Christensen, J.C. Wain, T.J. Lynch, K. Vernovsky, E.J. Mark, M. Lanuti, A.J. Iafrate, M. Mino-Kenudson, J.A. Engelman, Genotypic and histological evolution of lung cancers acquiring resistance to EGFR inhibitors, Sci. Transl. Med. 3 (75) (2011) 75ra26.
[22] N. Turner, R. Grose, Fibroblast growth factor signalling: from development to cancer, Nat. Rev. Cancer 10 (2) (2010) 116–129.
[23] M.V. Dieci, M. Arnedos, F. Andre, J.C. Soria, Fibroblast growth factor receptor inhibitors as a cancer treatment: from a biologic rationale to medical perspectives, Cancer Discov. 3 (3) (2013) 264–279.
[24] Y.K. Chae, K. Ranganath, P.S. Hammerman, C. Vaklavas, N. Mohindra, A. Kalyan, M. Matsangou, R. Costa, B. Carneiro, V.M. Villaflor, M. Cristofanilli, F.J. Giles, Inhibition of the fibroblast growth factor receptor (FGFR) pathway: the current landscape and barriers to clinical application, Oncotarget 8 (9) (2017) 16052–16074.
[25] K. Azuma, A. Kawahara, K. Sonoda, K. Nakashima, K. Tashiro, K. Watari, H. Izumi, M. Kage, M. Kuwano, M. Ono, T. Hoshino, FGFR1 activation is an escape mechanism in human lung cancer cells resistant to afatinib, a pan-EGFR family kinase inhibitor, Oncotarget 5 (15) (2014) 5908–5919.
[26] H. Terai, K. Soejima, H. Yasuda, S. Nakayama, J. Hamamoto, D. Arai, K. Ishioka, K. Ohgino, S. Ikemura, T. Sato, S. Yoda, R. Satomi, K. Naoki, T. Betsuyaku, Activation of the FGF2-FGFR1 autocrine pathway: a novel mechanism of acquired resistance to gefitinib in NSCLC, Mol. Cancer Res. 11 (7) (2013) 759–767.
[27] K.J. Gammelgaard, J. Vad-Nielsen, M.S. Clement, S. Weiss, T.F. Daugaard, F. Dagnæs-Hansen, P. Meldgaard, B.S. Sorensen, A.L. Nielsen, Upregulated FGFR1 expression as a mediator of intrinsic TKI resistance in EGFR-mutated NSCLC, Transl. Oncol. 12 (3) (2018) 432–440.
[28] V.D. Acevedo, R.D. Gangula, K.W. Freeman, R. Li, Y. Zhang, F. Wang, G.E. Ayala, L.E. Peterson, M. Ittmann, D.M. Spencer, Inducible FGFR-1 activation leads to irreversible prostate adenocarcinoma and an epithelial-to-mesenchymal transition, Cancer Cell 12 (6) (2007) 559–571.
[29] W.S. Brown, L. Tan, A. Smith, N.S. Gray, M.K. Wendt, Covalent targeting of fibroblast growth factor receptor inhibits metastatic breast Cancer, Mol. Cancer Ther. 15 (9) (2016) 2096–2106.
[30] K. Wang, W. Ji, Y. Yu, Z. Li, X. Niu, W. Xia, S. Lu, FGFR1-ERK1/2-SOX2 axis promotes cell proliferation, epithelial-mesenchymal transition, and metastasis in FGFR1-amplified lung cancer, Oncogene 37 (39) (2018) 5340–5354.
[31] J. Vad-Nielsen, A.L. Nielsen, Y. Luo, Simple method for assembly of CRISPR synergistic activation mediator gRNA expression array, J. Biotechnol. 274 (2018) 54–57.
[32] S. Konermann, M.D. Brigham, A.E. Trevino, J. Joung, O.O. Abudayyeh, C. Barcena, P.D. Hsu, N. Habib, J.S. Gootenberg, H. Nishimasu, O. Nureki, F. Zhang, Genome-scale transcriptional activation by an engineered CRISPR-Cas9 complex, Nature 517 (7536) (2015) 583–588.
[33] R. Thomsen, C.A. Solvsten, T.E. Linnet, J. Blechingberg, A.L. Nielsen, Analysis of qPCR data by converting exponentially related Ct values into linearly related X0 values, J. Bioinform. Comput. Biol. 8 (5) (2010) 885–900.
[34] Y.K. Chae, S. Chang, T. Ko, J. Anker, S. Agte, W. Iams, W.M. Choi, K. Lee, M. Cruz, Epithelial-mesenchymal transition (EMT) signature is inversely associated with T-cell infiltration in non-small cell lung cancer (NSCLC), Sci. Rep. 8 (1) (2018) 2918.
[35] D.L. Gibbons, C.J. Creighton, Pan-cancer survey of epithelial-mesenchymal transition markers across the cancer genome Atlas, Dev. Dyn. 247 (3) (2018) 555–564.
[36] I.M. Shapiro, A.W. Cheng, N.C. Flytzanis, M. Balsamo, J.S. Condeelis, M.H. Oktay, C.B. Burge, F.B. Gertler, An EMT-driven alternative splicing program occurs in human breast cancer and modulates cellular phenotype, PLoS Genet. 7 (8) (2011) e1002218.
[37] S.V. Litvinov, M. Balzar, M.J. Winter, H.A. Bakker, I.H. Briaire-de Bruijn, F. Prins, G.J. Fleuren, S.O. Warnaar, Epithelial cell adhesion molecule (Ep-CAM) modulates cell-cell interactions mediated by classic cadherins, J. Cell Biol. 139 (5) (1997) 1337–1348.
[38] C.J. Groger, M. Grubinger, T. Waldhor, K. Vierlinger, W. Mikulits, Meta-analysis of gene expression signatures defining the epithelial to mesenchymal transition during cancer progression, PLoS One 7 (12) (2012) e51136.
[39] R.M. Gemmill, J. Roche, V.A. Potiron, P. Nasarre, M. Mitas, C.D. Coldren, B.A. Helfrich, E. Garrett-Mayer, P.A. Bunn, H.A. Drabkin, ZEB1-responsive genes in non-small cell lung cancer, Cancer Lett. 300 (1) (2011) 66–78.
[40] M. Krentz Gober, J.P. Collard, K. Thompson, E.P. Black, A microRNA signature of response to erlotinib is descriptive of TGFbeta behaviour in NSCLC, Sci. Rep. 7 (1) (2017) 4202.
[41] H. Sato, K. Shien, S. Tomida, K. Okayasu, K. Suzawa, S. Hashida, H. Torigoe, M. Watanabe, H. Yamamoto, J. Soh, H. Asano, K. Tsukuda, S. Miyoshi, S. Toyooka, Targeting the miR-200c/LIN28B axis in acquired EGFR-TKI resistance non-small cell lung cancer cells harboring EMT features, Sci. Rep. 7 (2017) 40847.
[42] T. Yoshida, L. Song, Y. Bai, F. Kinose, J. Li, K.C. Ohaegbulam, T. Munoz-Antonia, X. Qu, S. Eschrich, H. Uramoto, F. Tanaka, P. Nasarre, R.M. Gemmill, J. Roche, H.A. Drabkin, E.B. Haura, ZEB1 mediates acquired resistance to the epidermal growth factor receptor-tyrosine kinase inhibitors in non-small cell lung cancer, PLoS One 11 (1) (2016) e0147344.
[43] A.F. Lee, M.C. Chen, C.J. Chen, C.J. Yang, M.S. Huang, Y.P. Liu, Reverse epithelial-mesenchymal transition contributes to the regain of drug sensitivity in tyrosine kinase inhibitor-resistant non-small cell lung cancer cells, PLoS One 12 (7) (2017) e0180383.
[44] T. Ohira, R.M. Gemmill, K. Ferguson, S. Kusy, J. Roche, E. Brambilla, C. Zeng, A. Baron, L. Bemis, P. Erickson, E. Wilder, A. Rustgi, J. Kitajewski, E. Gabrielson, R. Bremnes, W. Franklin, H.A. Drabkin, WNT7a induces E-cadherin in lung cancer cells, Proc. Natl. Acad. Sci. U. S. A. 100 (18) (2003) 10429–10434.
[45] Y. Takeyama, M. Sato, M. Horio, T. Hase, K. Yoshida, T. Yokoyama, H. Nakashima, N. Hashimoto, Y. Sekido, A.F. Gazdar, J.D. Minna, M. Kondo, Y. Hasegawa, Knockdown of ZEB1, a master epithelial-to-mesenchymal transition (EMT) gene, suppresses anchorage-independent cell growth of lung cancer cells, Cancer Lett. 296 (2) (2010) 216–224.
[46] J.E. Larsen, V. Nathan, J.K. Osborne, R.K. Farrow, D. Deb, J.P. Sullivan, P.D. Dospoy, A. Augustyn, S.K. Hight, M. Sato, L. Girard, C. Behrens, I.I. Wistuba, A.F. Gazdar, N.K. Hayward, J.D. Minna, ZEB1 drives epithelial-to-mesenchymal transition in lung cancer, J. Clin. Invest. 126 (9) (2016) 3219–3235.
[47] C.P. Bracken, P.A. Gregory, N. Kolesnikoff, A.G. Bert, J. Wang, M.F. Shannon, G.J. Goodall, A double-negative feedback loop between ZEB1-SIP1 and the microRNA-200 family regulates epithelial-mesenchymal transition, Cancer Res. 68 (19) (2008) 7846–7854.
[48] K. Holzmann, T. Grunt, C. Heinzle, S. Sampl, H. Steinhoff, N. Reichmann, M. Kleiter, M. Hauck, B. Marian, Alternative splicing of fibroblast growth factor receptor IgIII loops in cancer, J. Nucleic Acids 2012 (2012) 950508.
[49] C. Wuechner, A.C. Nordqvist, A. Winterpacht, B. Zabel, M. Schalling, Developmental expression of splicing variants of fibroblast growth factor receptor 3 (FGFR3) in mouse, Int. J. Dev. Biol. 40 (6) (1996) 1185–1188.
[50] A. Orr-Urtreger, M.T. Bedford, T. Burakova, E. Arman, Y. Zimmer, A. Yayon, D. Givol, P. Lonai, Developmental localization of the splicing alternatives of fibroblast growth factor receptor-2 (FGFR2), Dev. Biol. 158 (2) (1993) 475–486.
[51] V.P. Eswarakumar, I. Lax, J. Schlessinger, Cellular signaling by fibroblast growth factor receptors, Cytokine Growth Factor Rev. 16 (2) (2005) 139–149.
[52] Q. Zhao, O.L. Caballero, I.D. Davis, E. Jonasch, P. Tamboli, W.K. Yung, J.N. Weinstein, T.r.n. Kenna Shaw for, R.L. Strausberg, J. Yao, Tumor-specific isoform switch of the fibroblast growth factor receptor 2 underlies the mesenchymal and malignant phenotypes of clear cell renal cell carcinomas, Clin. Cancer Res. 19 (9) (2013) 2460–2472.
[53] S. Oltean, B.S. Sorg, T. Albrecht, V.I. Bonano, R.M. Brazas, M.W. Dewhirst, M.A. Garcia-Blanco, Alternative inclusion of fibroblast growth factor receptor 2 exon IIIc in Dunning prostate tumors reveals unexpected epithelial mesenchymal plasticity, Proc. Natl. Acad. Sci. U. S. A. 103 (38) (2006) 14116–14121.
[54] D. Ranieri, B. Rosato, M. Nanni, A. Magenta, F. Belleudi, M.R. Torrisi, Expression of the FGFR2 mesenchymal splicing variant in epithelial cells drives epithelial-mesenchymal transition, Oncotarget 7 (5) (2016) 5440–5460.
[55] H. Fischer, N. Taylor, S. Allerstorfer, M. Grusch, G. Sonvilla, K. Holzmann, U. Setinek, L. Elbling, H. Cantonati, B. Grasl-Kraupp, C. Gauglhofer, B. Marian, M. Micksche, W. Berger, Fibroblast growth factor receptor-mediated signals contribute to the malignant phenotype of non-small cell lung cancer cells: therapeutic implications and synergism with epidermal growth factor receptor inhibition, Mol. Cancer Ther. 7 (10) (2008) 3408–3419.
[56] E.L. Gottgens, P.N. Span, M.M. Zegers, Roles and regulation of epithelial splicing regulatory proteins 1 and 2 in Epithelial-Mesenchymal transition, Int. Rev. Cell Mol. Biol. 327 (2016) 163–194.
[57] C.C. Warzecha, R.P. Carstens, Complex changes in alternative pre-mRNA splicing play a central role in the epithelial-to-mesenchymal transition (EMT), Semin. Cancer Biol. 22 (5-6) (2012) 417–427.
[58] F. Malchers, F. Dietlein, J. Schottle, X. Lu, L. Nogova, K. Albus, L. Fernandez-Cuesta, J.M. Heuckmann, O. Gautschi, J. Diebold, D. Plenker, M. Gardizi, M. Scheffler, M. Bos, D. Seidel, F. Leenders, A. Richters, M. Peifer, A. Florin, P.S. Mainkar, N. Karre, S. Chandrasekhar, J. George, S. Silling, D. Rauh, T. Zander, R.T. Ullrich, H.C. Reinhardt, F. Ringeisen, R. Buttner, L.C. Heukamp, J. Wolf, R.K. Thomas, Cell-autonomous and non-cell-autonomous mechanisms of transformation by amplified FGFR1 in lung cancer, Cancer Discov. 4 (2) (2014) 246–257.